# Inflammation induces lymphangiogenesis through up-regulation of VEGFR-3 mediated by NF-κB and Prox1

Michael J. Flister,[1] Andrew Wilber,[1,2] Kelly L. Hall,[1] Caname Iwata,[3] Kohei Miyazono,[3] Riccardo E. Nisato,[4] Michael S. Pepper,[5] David C. Zawieja,[6] and Sophia Ran[1]

Departments of [1]Medical Microbiology, Immunology, and Cell Biology and [2]Surgery, Southern Illinois University School of Medicine, Springfield; [3]Department of Molecular Pathology, Graduate School of Medicine, University of Tokyo, Tokyo, Japan; [4]Department of Cell Physiology and Metabolism, University Medical Center, Geneva, Switzerland; [5]Netcare Institute of Cellular and Molecular Medicine, Pretoria, South Africa; and [6]Department of Systems Biology and Translational Medicine, Cardiovascular Research Institute, Texas A&M Health Science Center, College Station

The concept of inflammation-induced lymphangiogenesis (ie, formation of new lymphatic vessels) has long been recognized, but the molecular mechanisms remained largely unknown. The 2 primary mediators of lymphangiogenesis are vascular endothelial growth factor receptor-3 (VEGFR-3) and Prox1. The key factors that regulate inflammation-induced transcription are members of the nuclear factor-kappaB (NF-κB) family; however, the role of NF-κB in regulation of lymphatic-specific genes has not been defined. Here, we identified VEGFR-3 and Prox1 as downstream targets of the NF-κB pathway. In vivo time-course analysis of inflammation-induced lymphangiogenesis showed activation of NF-κB followed by sequential up-regulation of Prox1 and VEGFR-3 that preceded lymphangiogenesis by 4 and 2 days, respectively. Activation of NF-κB by inflammatory stimuli also elevated Prox1 and VEGFR-3 expression in cultured lymphatic endothelial cells, resulting in increased proliferation and migration. We also show that Prox1 synergizes with the p50 of NF-κB to control VEGFR-3 expression. Collectively, our findings suggest that induction of the NF-κB pathway by inflammatory stimuli activates Prox1, and both NF-κB and Prox1 activate the VEGFR-3 promoter leading to increased receptor expression in lymphatic endothelial cells. This, in turn, enhances the responsiveness of pre-existing lymphatic endothelium to VEGFR-3 binding factors, VEGF-C and VEGF-D, ultimately resulting in robust lymphangiogenesis. (Blood. 2010;115: 418-429)

## Introduction

The lymphatic vascular system has multiple functions in normal physiology including regulation of interstitial pressure,[1] lipid absorption,[2] immune surveillance,[1] and resolution of inflammation.[3] The formation of new lymphatic vessels (ie, lymphangiogenesis) is dynamic during embryogenesis but is relatively rare and selectively regulated in adulthood. Insufficient development of postnatal lymphatic vessels impairs immune function and causes tissue edema,[1] whereas excessive lymphangiogenesis is associated with malignancy and strongly implicated in lymphatic metastasis.[4]

The key protein that regulates lymphangiogenesis is vascular endothelial growth factor receptor-3 (VEGFR-3),[5] a tyrosine kinase receptor expressed primarily in lymphatic endothelial cells (LECs).[6] VEGFR-3 signaling is activated upon binding of vascular endothelial growth factor-C (VEGF-C) or the related factor, VEGF-D.[5] In adulthood, lymphangiogenesis and elevated VEGFR-3 expression coincide with inflammatory conditions including cancer,[7] wound healing,[8] and chronic inflammatory diseases. Increased lymphatic vessel density (LVD) has been documented in chronic airway infection,[9] psoriasis,[10] arthritis,[11] and corneal injury.[12] VEGF-C and VEGF-D are elevated during inflammation, being produced by a variety of cells residing at inflamed sites, including macrophages,[9,13,14] dendritic cells, neutrophils,[9] mast cells, fibroblasts,[15] and tumor cells.[14] Inflammation-induced lymphatic hyperplasia and lymphangiogenesis are likely the result of increased VEGFR-3 expression that amplifies response to VEGF-C/-D. This is supported by observations that blocking VEGFR-3 signaling inhibits lymphangiogenesis during chronic inflammation,[9] wound healing,[16] and malignancy.[17]

Lymphangiogenesis is also regulated by the lymphatic-specific transcription factor, Prospero-related homeobox-1 (Prox1)[18,19] that specifies LEC fate by regulating expression of VEGFR-3[19] and other lymphatic-specific proteins during embryogenesis. The central role of Prox1 in developmental lymphangiogenesis suggests a similar role for Prox1 in adulthood. Studies have shown that Prox1 induces VEGFR-3 in adult blood vascular endothelial cells (BECs),[18,20] whereas silencing Prox1 in adult LECs down-regulates VEGFR-3 expression.[20,21] Prox1 has been shown to be up-regulated by inflammatory cytokines[22] and to colocalize with VEGFR-3 in lymphatic vessels. However, the role of Prox1 in regulation of VEGFR-3 expression during inflammation in vivo is unknown.

The primary mediators of the inflammatory response are dimeric transcription factors that belong to the nuclear factor-kappaB (NF-κB) family consisting of RelA (p65), NF-κB1 (p50), RelB, c-Rel, and NF-κB2 (p52).[23] The main NF-κB protein complexes that regulate the transcription of responsive genes are p50/p65 heterodimers or p50 and p65 homodimers.[24] More than

---

450 NF-κB–inducible genes have been identified, including proteins that mediate inflammation, immunity, tumorigenesis, and angiogenesis.[23] Several NF-κB–regulated genes stimulate lymphangiogenesis either directly (eg, VEGF-A[25] and VEGF-C[26]) or indirectly, by up-regulating VEGF-C and VEGF-D (eg, IL-1β,[15] TNF-α,[15] and COX-2[14]). Activated NF-κB signaling coincides with increased VEGFR-3+ lymphatics during inflammation,[9] suggesting a role for NF-κB in regulation of VEGFR-3 expression.

Although extensive evidence supports the link between inflammation and lymphangiogenesis, the molecular mechanisms underlying this association are largely unknown. We postulate that NF-κB, the main intracellular mediator of inflammation, regulates transcription of key mediators of lymphangiogenesis, VEGFR-3 and Prox1. To test this hypothesis, we used a mouse model of inflammatory peritonitis,[14] which showed that lymphangiogenesis is preceded by increased VEGFR-3 and Prox1 expression on preexisting inflamed lymphatic vessels. Analysis of the human VEGFR-3 promoter showed transcriptional regulation by p50, p65, and Prox1. These data demonstrate for the first time that NF-κB and Prox1 induce VEGFR-3 transcription, indicating the important roles for both factors in the regulation of VEGFR-3–dependent inflammatory lymphangiogenesis in vivo.

## Methods

### Materials

Human Prox1 CDS ligated into pCMV6-XL6 (pCMV-Prox1) plasmid was purchased from OriGene. NF-κB plasmids, pCMV-Flag-p50 and pCMV-Flag-p65, were kindly provided by Dr Albert Baldwin (University of North Carolina, Chapel Hill). Promoter-luciferase reporter plasmids for ubiquitin C and phosphoglycerate kinase were described previously.[27] Lipopolysaccharide (LPS) was purchased from Sigma-Aldrich. Rat VEGFR-3–specific ligand, VEGF-C152S, and human interleukin-3 (IL-3) were purchased from Peprotech. Pyrrolidine dithiocarbamate (PDTC) and MG-132 were purchased from Calbiochem. Leptomycin B was from LC Laboratories.

### Antibodies

Primary antibodies used in this study were: goat anti–mVEGFR-3 and anti-Prox1 (R&D Systems); rabbit anti-p65, anti-pp65, anti-p50, and anti-pp50 (Santa Cruz); rabbit anti–mLYVE-1 and anti-Prox1 (AngioBio); rabbit anti–Ki-67 (Biomeda); goat anti–acetylated-histone-H3 (Upstate); mouse anti-Flag (ABM); mouse anti-β-actin (JLA20; Developmental Studies Hybridoma Bank); and rabbit anti–VEGF-C (Invitrogen). Secondary horseradish peroxidase–, fluorescein isothiocyanate–, and Cy3-conjugated donkey anti–rabbit and anti–goat antibodies and nonspecific rabbit immunoglobulin G (IgG) were from Jackson ImmunoResearch Laboratories.

### Cell lines

Rat LECs (RLECs) were isolated and cultured as previously described.[28] Human embryonic kidney cells (HEK293) were cultured in Dulbecco modified Eagle medium (DMEM) with 10% fetal bovine serum (FBS). Human primary LECs (H-LLY) and immortalized human dermal LECs (HDLEC$_{htert}$)[29] were cultured in gelatin-coated flasks in microvascular endothelial cell growth medium-2 (EGM-2MV) medium (Clonetics). Human lung microvascular endothelial cells (HULECs) were obtained from the Centers for Disease Control and Prevention.

### Mouse peritonitis model

All mice experiments were approved by Southern Illinois University School of Medicine Institutional Laboratory Animal Care and Use Committee. Female BALB/c mice (3-6 months) were obtained from The Jackson Laboratory and treated in accordance with institutional guidelines. Peritonitis was induced by 0.5-mL intraperitoneal injections of 1.5% sodium thioglycollate (vol/vol in saline; BD Biosciences) for 2 weeks, as previously described.[14] For time-course analysis, mice (3-4 per group) received thioglycollate (TG) every 48 hours for the indicated periods. Control mice were injected intraperitoneally with 0.5 mL of saline. Diaphragms were removed after a 2-week treatment, fixed with 10 N of Mildform for 1 hour at room temperature, bathed in 30% sucrose overnight, and snap-frozen.

### Immunohistochemistry

Frozen 8-μm sections were fixed with acetone for 10 minutes, washed in phosphate-buffered saline plus Tween-20 (pH 7.4, 0.1% Tween-20) for 10 minutes and incubated for 1 hour at 37°C with primary antibodies (diluted 1:100) against VEGFR-3, LYVE-1, Prox1, or Ki-67, followed by appropriate fluorescein isothiocyanate– or Cy3-conjugated secondary antibodies (diluted 1:100) for 1 hour at 37°C. For double immunofluorescent staining, sections were incubated with each primary and secondary antibody for 1 hour at 37°C and washed for 10 minutes in phosphate-buffered saline plus Tween-20 between steps. Slides were mounted in Vectashield medium containing 4,6′-diamidino-2-phenylindole (4,6 diamidino-2-phenylindole) nuclear stain (Vector Labs). Images were acquired on an Olympus BX41 upright microscope equipped with a DP70 digital camera and DP Controller software (Olympus).

### Immunofluorescent intensity measurements

Analysis of VEGFR-3 and LYVE-1 double-staining was performed as described by Tammela et al,[30] with slight modifications. In brief, diaphragm sections were double-stained with goat anti–mVEGFR-3 and rabbit anti–mLYVE-1 antibodies. Fluorescent images were acquired at a constant exposure time at 400× magnification on an Olympus IX71 inverted microscope (Olympus) equipped with a Retiga Exi charge-coupled device camera (QImaging). Diaphragms stained with secondary antibodies alone were used to set the exposure time. Images acquired at a constant exposure time were converted to 12-bit gray scale followed by outlining vascular structures and analysis with Image-Pro Software (Media Cybernetics). Supplemental Figure 1 (available on the *Blood* website; see the Supplemental Materials link at the top of the online article) shows an example of image acquisition and vessel outlining. All images were within a linear intensity range between 0 and 4095. To exclude nonspecific staining, structures less than 10 μm (1 μm = 6.4 pixels) in diameter were excluded. To calculate mean vessel intensity, the sums of pixel intensities per vessel were divided by total vessel area (μm²). Mean vessel intensities from 5 to 10 images per diaphragm (n = 3 per group) were averaged and compared between treated and control groups.

### Western blot analysis

Cells were lysed in ice-cold buffer [50mM tris (hydroxymethyl)aminomethane-HCl, pH 7.5, 150mM NaCl, 1mM ethylenediaminetetraacetic acid, 1% Triton-X100, 0.1% sodium dodecyl sulfate, phenylmethylsulphonyl fluoride 1:100, and protease inhibitor cocktail 1:50]. Proteins separated in 12% sodium dodecyl sulfate–polyacrylamide gel were transferred onto nitrocellulose membranes followed by overnight incubation with primary antibodies against p50, p65, Prox1, LYVE-1, VEGFR-3, Flag-tag, or β-actin; 1-hour incubation with horseradish peroxidase–conjugated secondary antibodies; and development with enhanced chemiluminescence reagent (Pierce). Protein bands were visualized using a Fujifilm LAS-3000 camera and analyzed with Image-Reader LAS-3000 software.

### VEGFR-3 promoter cloning

Segments of −849 bp, −514 bp, −341 bp, −331 bp, −118 bp, and −46 bp of the 5′ untranslated region of VEGFR-3 and +55 bp of exon 1 were amplified by polymerase chain reaction (PCR) from a human genomic bacterial artificial chromosome (BAC) clone, CTD-2546M13 (Open Biosystems). Promoter segments spanning −436/−254 bp and −849/−254 bp (Δ309) were also PCR-amplified. Products were cloned into the pGL4 basic vector (Promega) to produce VEGFR-3 promoter-luciferase constructs. All

clones were sequenced and verified through comparison with published genomic sequence. Human VEGFR-3 promoter sequence (GenBank accession no. DQ911346[31]) was analyzed using MatInspector (http://www.genomatix.de/products/MatInspector/index.html[32]) and compared with published transcription factor binding sites.

## Assay for VEGFR-3 promoter activity

Cells were transfected with 1 μg of DNA composed of 0.96 μg of promoter construct and 0.04 μg of Herpes simplex thymidine-kinase promoter–driven renilla luciferase (Promega) mixed with 3 μL of ExGen500 (Fermentas). After 24 hours, cells were lysed with 0.2% Triton-X100, and firefly and renilla luciferase activities were measured by a dual-luciferase assay performed according to manufacturer's protocol. Promoter-firefly luciferase activity was normalized per renilla activity or milligram of total protein.

## Inflammatory stimulation of LECs

HDLECs$_{htert}$ were seeded in 6-well plates (200 000 cells/well) in 0.5% EGM2 medium (Lonza). Medium was replaced daily during a 72-hour time period, before treatment with IL-3 (10 ng/mL) or LPS (100 ng/mL) for 6 or 24 hours. RNA extraction and analysis of transcripts by quantitative reverse-transcription (qRT)–PCR was performed as described in "RT-PCR and qRT-PCR."

## Cell proliferation and migration assays

RLECs were seeded in DMEM containing 1.5% FBS in 24-well plates at the density of 50 000 cells/well. IL-3 (5-100 ng/mL), LPS (50-1000 ng/mL), and VEGF-C152S (25-200 ng/mL) were added 2 hours after seeding. The effect of combined cytokines was measured after stimulation with VEGF-C152S (100 ng/mL) mixed with IL-3 (10 ng/mL) or LPS (500 ng/mL). After 72-hour incubation, cells were trypsinized and enumerated. The results are presented as the averaged cell number per well derived from 3 experiments performed in triplicate plus or minus SEM.

Cell migration was measured using 8 μm-pore Transwells according to the manufacturer's protocol (Corning). In brief, 50 000 RLECs were seeded in 0.25% DMEM on pre-equilibrated inserts. IL-3 (10 ng/mL), LPS (500 ng/mL), VEGF-C152S (200 ng/mL), or 0.25% FBS (negative control) was added to bottom chambers. After 24-hour incubation, inserts were washed, fixed in 2% paraformaldehyde for 10 minutes, and stained by crystal violet. Numbers of cells migrated per field were determined on 6 random images acquired at 200× and averaged.

## ChIP

RLECs ($2 \times 10^7$) were grown to 90% confluence and fixed with 1% formaldehyde. Cell lysis, shearing, and chromatin immunoprecipitation (ChIP) were performed using a ChIP-IT Express Kit according to the manufacturer's protocol (Active Motif). Chromatin was precipitated with anti-p50, p65, Prox1, acetylated-histone-H3 antibodies, or nonspecific rabbit IgG (negative control). Precipitated chromatin was amplified by PCR using primers for rat VEGFR-3 promoter listed in supplemental Table 1.

## Suppression of p50/p65 expression by siRNA

Previously validated 21-nucleotide-long siRNA duplexes against p50 (sense strand, 5′-GGGGCUAUAAUCCUGGACUdTdT-3′)[33] and p65 (sense strand, 5′-GCCCUAUCCCUUUACGUCAdTdT-3′)[34] (Dharmacon) and predesigned Silencer Negative Control no. 1 siRNA (Ambion) were used for suppression of p50 and p65 expression. H-LLY cells were transfected with siRNA for 16 hours using siPORT NeoFX (Ambion) according to the manufacturer's protocol. Total RNA was isolated 48 hours after transfection and transcript levels were determined by qRT-PCR.

## RT-PCR and qRT-PCR

Total RNA extracted by Tri-reagent was reverse transcribed using RTG You-Prime Reaction beads (Amersham) and random hexamer primers (Invitrogen). All primers used in this study are listed in supplemental Table 1. End point RT-PCR analysis was performed as previously described,[7] then visualized and analyzed using a FluroChem5500 imager (AlphaInnotech). qRT-PCR was performed using SYBR Master Mix and a 7500 Real-Time PCR machine from Applied Biosystems. Data were normalized to β-actin and relative mRNA expression was determined using the ΔΔCt method.

## Statistical analysis

Statistical analysis was performed using SAS software (SAS Institute Inc). All results are expressed as mean plus or minus SEM. Differences in lymphatic vessel densities between groups were assessed by unpaired Student $t$ test or Wilcoxon rank sum test. Intensity of VEGFR-3 and LYVE-1 staining per lymphatic vessels was assessed by analysis of variance for a nested design. Statistical significance was defined as $P$ value less than .05.

# Results

## Inflammation induces lymphatic VEGFR-3 and Prox1 expression during lymphangiogenesis in vivo

Regulation of VEGFR-3 by inflammation is suggested by reports demonstrating inhibition of lymphangiogenesis by blockade of VEGFR-3 signaling.[9] Prox1 may also contribute to this process because it is induced by inflammatory mediators,[22] which coincides with elevated VEGFR-3.[35] However, the roles of VEGFR-3 and Prox1 in inflammatory lymphangiogenesis have not been demonstrated.

To analyze VEGFR-3 and Prox1 expression during inflammation, we induced peritonitis in Balb/c mice by TG injections, a method reported to induce lymphangiogenesis in the diaphragm.[14] Diaphragms from saline (control)– and TG-treated mice were removed after a 2-week treatment and stained for the lymphatic marker, LYVE-1, and VEGFR-3 (Figure 1). Consistent with previous studies,[14,36] the number of LYVE-1⁺ lymphatic vessels increased by 1.9-fold ($\pm$ 0.3-fold) in TG-treated mice compared with controls (Figure 1A-B). These tissues also showed a 4.5-fold ($\pm$ 0.3-fold) increase in VEGFR-3⁺ vessel density (Figure 1A,C). Coexpression of VEGFR-3 and LYVE-1 was quantified using the method described by Tammela et al[30] that measures the fluorescent intensity of target expression normalized per vascular area. This revealed a lymphatic-specific increase of VEGFR-3 (~ 67%) but not LYVE-1 (Figure 1D-E, supplemental Figure 3) expression, suggesting that inflammation increases both LVD and VEGFR-3 expression per individual vessel.

Prox1 reportedly regulates VEGFR-3 expression in cultured LECs[18,20]; however, a similar function in vivo has not been reported. We sought to determine Prox1 expression in VEGFR-3⁺ lymphatic vessels during inflammation. Double-staining showed coincident up-regulation of VEGFR-3 and Prox1 in lymphatic vessels of inflamed diaphragms compared with control tissues (Figure 1F). Moreover, the frequency of Prox1⁺ nuclei per lymphatic vessel area was increased by 3.3-fold ($\pm$ 0.5-fold; Figure 1G).

To determine the proliferative status of VEGFR-3⁺/Prox1⁺ vessels, control and inflamed sections were costained for Ki-67 in combination with anti–VEGFR-3 or anti-Prox1 antibodies. Quiescent lymphatic vessels of control mice lacked Ki-67. In contrast, lymphatic vessels in TG-treated mice displayed widespread Ki-67 colocalized with both Prox1 and VEGFR-3 (Figure 1H). Collectively, these data demonstrate that inflammation induces VEGFR-3 and Prox1 expression on preexisting and sprouting lymphatic vessels.

**Figure 1. Inflammation induces VEGFR-3 and Prox1 expression in activated lymphatic vessels.** Peritonitis was induced by repetitive intraperitoneal injections of thioglycollate (TG) every 48 hours for 2 weeks. (A) Diaphragms from mice treated for 2 weeks with TG to induce peritonitis or saline as a control (n = 3 mice per group) were double-stained with anti–LYVE-1 and anti–VEGFR-3 antibodies. Note strong expression and complete overlap of VEGFR-3 with LYVE-1 in inflamed tissues compared with quiescent lymphatic vessels in control sections with weakly detected (arrow) or absent (arrowheads) VEGFR-3. LYVE-1^{+} (B) and VEGFR-3^{+} (C) lymphatic vessels were counted on the entire diaphragm sections and the numbers were normalized per total section area expressed in square millimeters. The results are presented as the mean vessel density per group ± SEM. (B) *$P < .05$ versus control as determined by Wilcoxon rank sum test. (C) **$P < .01$ versus control as determined by Student unpaired $t$ test. The mean fluorescent intensity (MFI) per vessel was analyzed on LYVE-1^{+} (D) and VEGFR-3^{+} (E) lymphatic vessels (5-10 vessels per diaphragm). MFI is expressed as relative units normalized per vascular area expressed in square micrometers. The mean MFI values ± SEM derived from 3 mice per group are shown. (E) *$P < .05$ versus control, as determined by nested analysis of variance described in "Statistical analysis." (F) Diaphragms from TG-treated and control mice were double-stained with anti-Prox1 and anti–VEGFR-3 antibodies. Arrows point to Prox1^{+} nuclei. (G) Prox1^{+} nuclei were enumerated and normalized per LYVE-1^{+} lymphatic area ($\mu$m$^2$) in diaphragms of TG- and saline-treated control mice. **$P < .01$ versus control as determined by Student unpaired $t$ test. (H) Diaphragm sections were costained with antibodies against VEGFR-3 or Prox1 and a proliferative marker, Ki-67, to assess proliferative status of lymphatic vessels in the diaphragms of TG-treated or control mice. Note overlapping expression of Ki-67/VEGFR-3 (arrow) and Ki-67/Prox1 (arrowhead) detected in inflamed lymphatic vessels but absent from quiescent lymphatic vessels in control tissues. Scale bars represent 100 $\mu$m (A) and 20 $\mu$m (F,H).
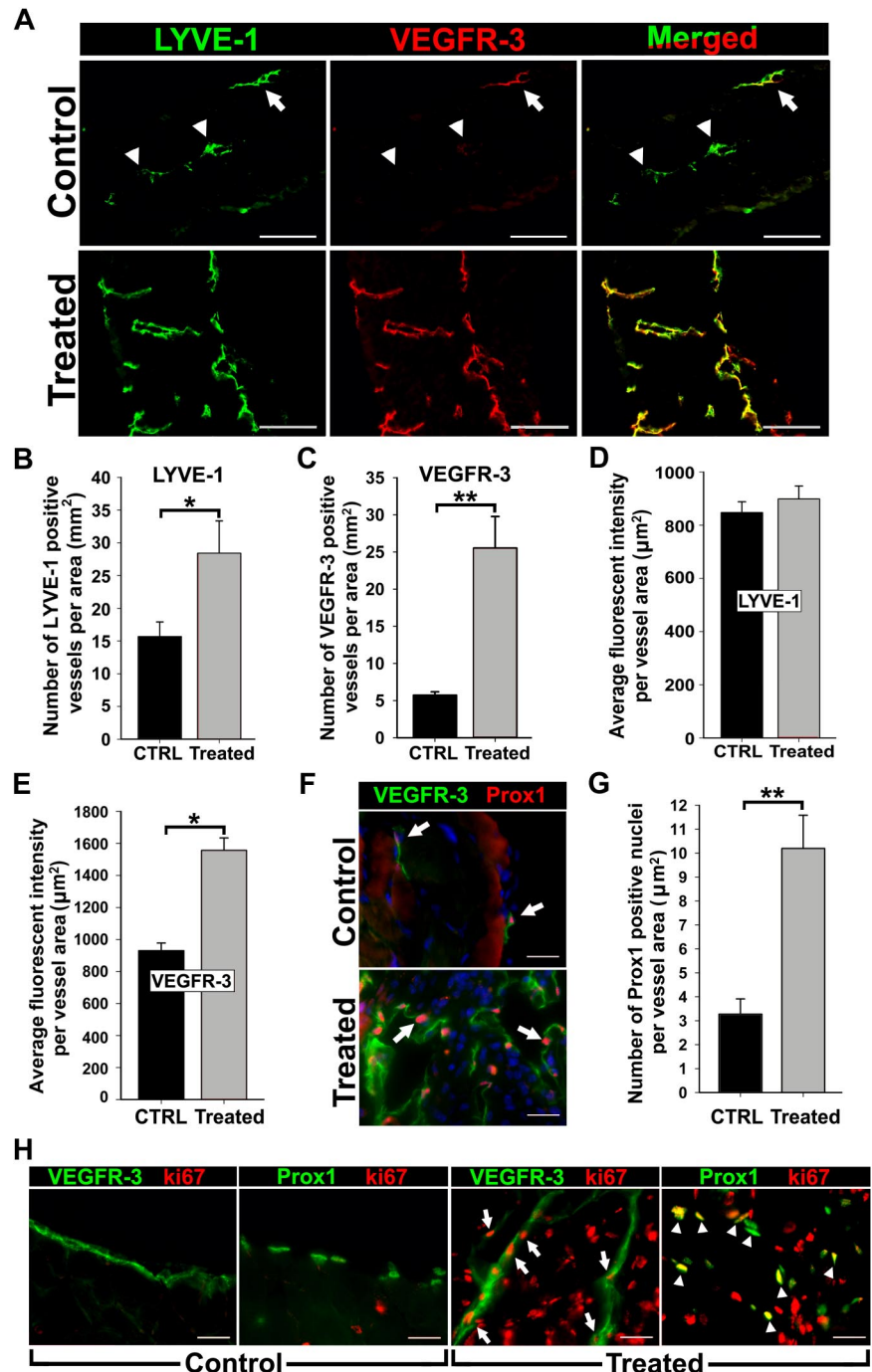
## Increased Prox1 and VEGFR-3 expression precedes lymphangiogenesis

LEC activation is associated with increased Prox1[37] and VEGFR-3,[5] yet their lymphatic-specific expression kinetics at early stages of lymphangiogenesis has not been examined. To determine the timeline of events leading to lymphangiogenesis, diaphragms from control and TG-treated mice harvested at days 1 to 4 and 7 after treatment were analyzed for expression of Prox1, VEGFR-3, and LYVE-1 by immunofluorescence and Western blot. Figure 2A and B show that compared with control tissues, the density of Prox1^{+} lymphatic vessels increased (3.8-fold, $P < .001$) on the first day and remained significantly elevated (2.2- to 3.1-fold) on days 2 to 7. In contrast, the increase in VEGFR-3^{+} vessel density

became statistically significant only on day 4 (1.7-fold, $P < .05$) and day 7 (3.1-fold, $P < .01$, Figure 2C). During this period, LYVE-1^{+} vessel density was unchanged except for an insignificant 1.6-fold increase on day 7 (Figure 2D). This immunofluorescent analysis showed that increased Prox1 expression precedes VEGFR-3 up-regulation by 2 to 3 days and elevation of both proteins precedes lymphangiogenesis.

Western blot analysis of actin-normalized protein expression of lymphatic markers as well as total and phosphorylated NF-κB p50 and p65 at different days after treatment confirmed this conclusion (Figure 2E). As expected, p50, p65, p-p50, and p-p65 were induced by inflammation with the most pronounced changes detected in p-p50 on the first day of treatment. NF-κB increase was mirrored
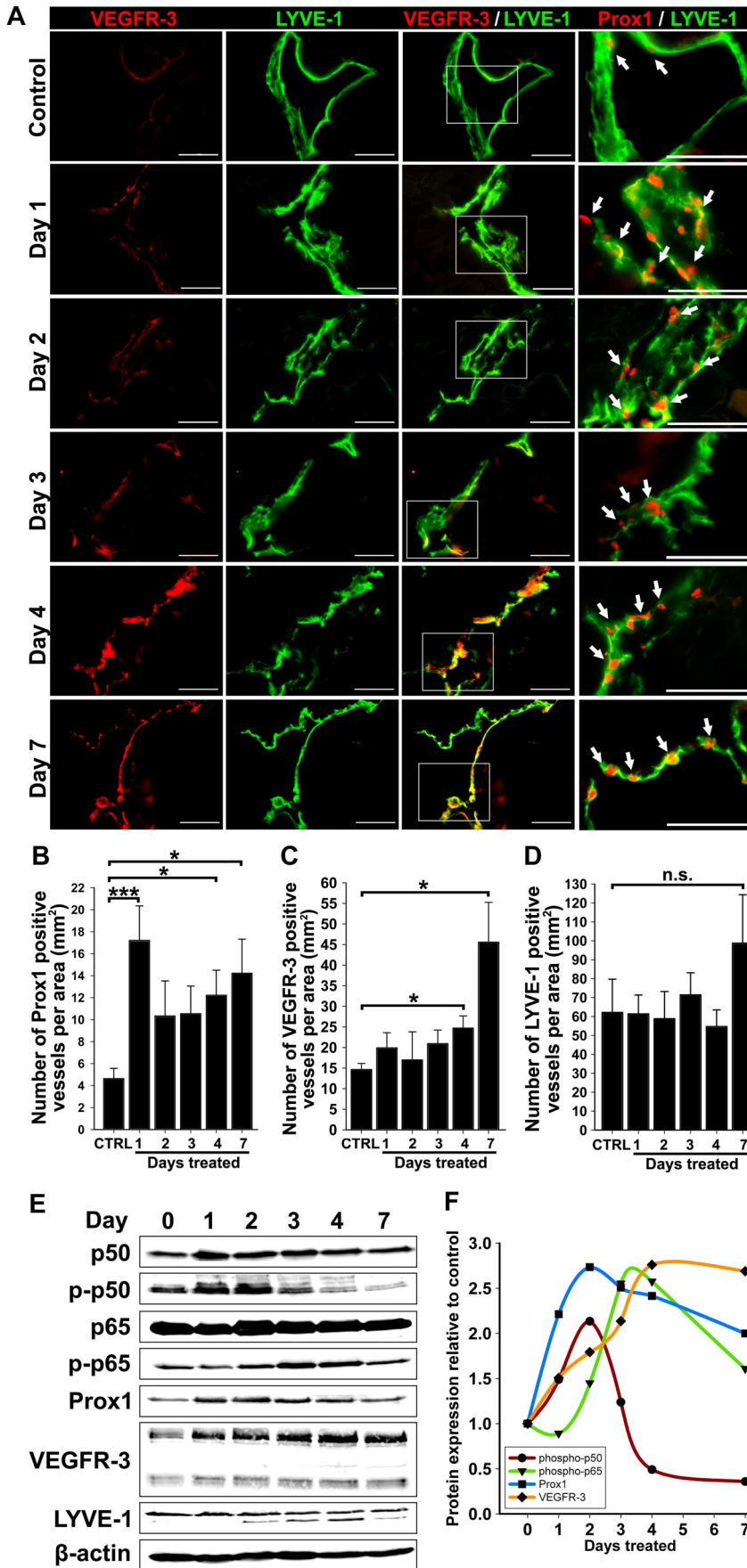
**Figure 2. Up-regulation of VEGFR-3 and Prox1 precedes new lymphatic vessel formation during inflammation.** (A) Double immunostaining of VEGFR-3/LYVE-1 and Prox1/LYVE-1 in serial diaphragm sections derived from mice treated with saline or TG (n = 3-4 mice per group) and harvested 1, 2, 3, 4, and 7 days after onset of treatment. Scale bars represent 50 μm. Lymphatic vessels shown are representative of whole diaphragm sections from 3 to 4 mice per group. (B-D) Quantification of Prox1-positive (B), VEGFR-3—positive (C), and LYVE-1—positive (D) vessels normalized per area of the entire diaphragm section measured in square millimeters. Quantitative analysis was performed on diaphragms harvested from 3 to 4 mice per group at indicated days after the first TG or saline injection. Data are presented as the mean number of vessels per diaphragm section ± SEM; ns denotes nonsignificant changes; $*P < .05$ and $***P < .01$ versus control, as determined by Student unpaired $t$ test. (E) Protein expression of Prox1, VEGFR-3, LYVE-1, NF-κB p50 phosphorylated on Ser337, nonphosphorylated NF-κB p50, NF-κB p65 phosphorylated on Ser276, nonphosphorylated NF-κB p65, and β-actin was determined by Western blot of combined lysates (100 μg of total protein per lane) derived from 3 to 4 mice per group. (F) Protein expression in Western blots was determined by band densitometry. Values were normalized to β-actin and are shown as fold increase relative to expression of corresponding proteins in untreated control mice at day 0.

**Figure 3. VEGFR-3 promoter characterization and gene expression in lymphatic endothelial cells.** (A) VEGFR-3 mRNA expression and (B) full-length VEGFR-3$^{-849/+55}$ promoter activity were measured in the lymphatic endothelial cell lines RLECs, H-LLY, and HDLECs$_{htert}$. Human lung blood microvascular endothelial cell line, HULEC, was used as a VEGFR-3–negative cell line. Data shown are a representative image of VEGFR-3 transcript expression of 3 independent experiments (A) and the mean promoter activity of 3 independent experiments ± SEM (B). **$P < .01$ versus VEGFR-3 promoter activity in the negative control cell line HULEC as determined by Student unpaired $t$ test. (C) Activities of VEGFR-3 promoter deletion constructs were tested in RLECs, H-LLY, and HDLECs$_{htert}$. The left panel shows schematic illustration of deletion constructs with relative locations of predicted transcription factor binding sites. The right panel shows VEGFR-3 promoter activity of deletion constructs presented as relative light units per second (RLU/S) normalized per renilla luciferase activity of cotransfected thymidine kinase (TK)–renilla plasmid. Experiments were performed in duplicate and reproduced at least 3 times. Data are presented as the mean promoter activity of 3 independent experiments ± SEM.
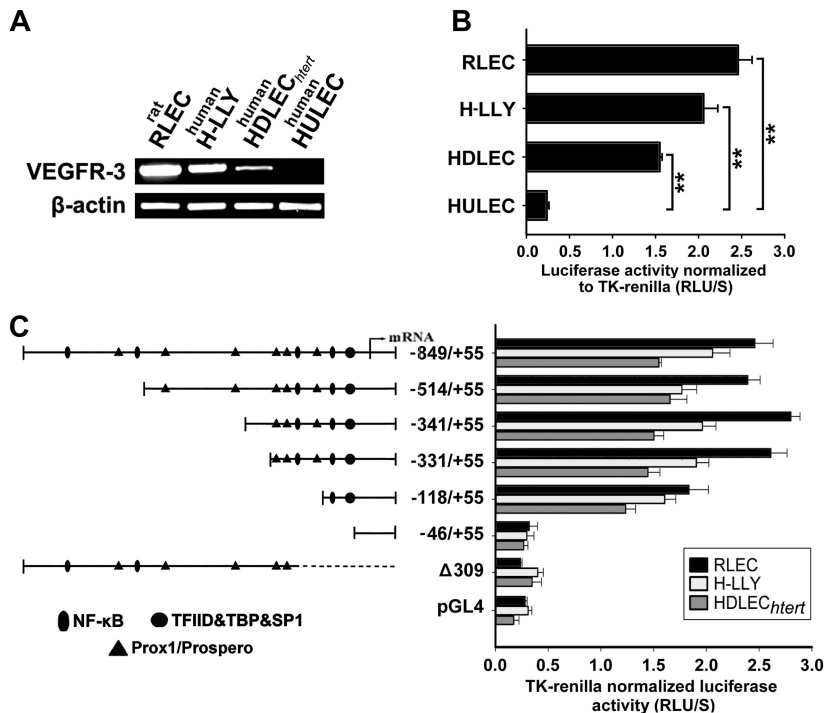
by Prox1 up-regulation that doubled on day 1 of inflammation and nearly tripled on day 2 (Figure 2F). In contrast, the peak of VEGFR-3 expression was delayed to day 4, on which its level in inflamed tissues was 2.8-fold higher compared with controls (supplemental Table 2). Consistent with immunostaining, no changes in LYVE-1 protein were detected over 7 days of treatment. These data suggest that activation of NF-κB and Prox1 might be responsible for LEC activation, VEGFR-3 elevation, and lymphangiogenesis. Because no significant changes in LVD were detected in the first week of inflammation, these findings imply that NF-κB, Prox1, and VEGFR-3 are all required for lymphangiogenesis that is preceded by up-regulation of these proteins by 3 to 5 days.

## Characterization of the human VEGFR-3 regulatory elements

To gain further insights into inflammation-dependent induction of VEGFR-3, we cloned and characterized the human VEGFR-3 promoter. Previous testing of the mouse VEGFR-3 promoter[38] demonstrated that the proximal 0.8 kb is sufficient to mediate cell type–specific transcriptional activity. However, NF-κB– and Prox1-dependent regulation of human or mouse promoter has not been previously examined.

High activity of the VEGFR-3$^{-849/+55}$ promoter was detected in 3 LEC lines with endogenous VEGFR-3 expression (Figure 3A). Promoter activity in LECs was 10.25-fold (± 0.7-fold; RLECs), 8.6-fold (± 0.7-fold; H-LLY), and 6.5-fold (± 0.2-fold; HDLECs$_{htert}$) higher than in the human blood vascular endothelial line, HULEC (Figure 3B). Promoter-reporter specificity was confirmed by empty vector and a promoter construct lacking the transcription start site (Δ309), both of which had 10% of the activity mediated by full-length VEGFR-3$^{-849/+55}$ (Figure 3C).

To identify the core elements required for transcriptional activity of the promoter we performed deletion analysis. Truncation from −849 bp to −331 bp did not significantly affect promoter activity (Figure 3C), suggesting that *cis*-acting response elements are located within the proximal −331/+55-bp region. Similar promoter activity was measured in human and rat LECs suggesting

that the regulatory elements are conserved among species. Analysis of the −331/+55-bp region identified putative binding sites for several transcription factors including NF-κB and Prox1. Promoter truncation from −331 bp to −118 bp reduced activity by 15% to 30%, whereas reduction to −46 bp reduced luciferase activity to the level of control Δ309 construct (Figure 3C). This suggested that NF-κB and Prox1, whose binding sites are located within the proximal −331-bp region, are responsible for up-regulation of VEGFR-3 observed in vivo.

## NF-κB transcription factors regulate VEGFR-3 expression in LECs

To determine the role of NF-κB in regulation of VEGFR-3 expression, LECs were cotransfected with the VEGFR-3$^{-849/+55}$ promoter and pCMV-Flag-p50, pCMV-Flag-p65, or empty plasmids. Equivalent expression of NF-κB subunits was determined by Western blot using Flag-specific antibody (supplemental Figure 4A). Compared with empty vector, NF-κB p65 activated VEGFR-3 promoter by 9-fold (± 1.0-fold) and 6-fold (± 0.5-fold) in H-LLY and RLECs, respectively. However, NF-κB p50 increased promoter activity by 58-fold (± 7-fold) and 51-fold (± 5-fold) in H-LLY and RLECs, respectively (Figure 4A). The difference in promoter activation was not due to functional deficiency of Flag-p65 construct as demonstrated by cotransfection with a NF-κB luciferase-reporter (supplemental Figure 4B). These data suggested that p50 has higher transactivation potential of VEGFR-3 promoter than p65 protein.

We used ChIP assay to determine whether NF-κB subunits bind the VEGFR-3 promoter. Primers were designed to encompass the region that includes or lacks the potential NF-κB sites. Only the −403/−238-bp promoter segment was detected by anti-p50, anti-p65, and anti–acetylated-H3 antibodies, indicating binding and active transcription by NF-κB in this region. ChIP analysis showed preferential binding by the p50 subunit (Figure 4B). Nonspecific rabbit IgG and primers flanking the region devoid of

NF-κB binding sites did not amplify PCR products, demonstrating specificity of the ChIP assay.

### Inflammatory stimuli induce LEC proliferation and migration via VEGFR-3 signaling

Because the VEGFR-3 promoter was activated by NF-κB factors, we reasoned that treatment of LECs with NF-κB–dependent



inflammatory mediators should increase the level of VEGFR-3 transcripts. To test this hypothesis, HDLECs$_{htert}$ were stimulated with known NF-κB activators, IL-3 (10 ng/mL) or LPS (100 ng/mL), for 6 and 24 hours, followed by qRT-PCR analysis of NF-κB p50 and p65, E-selectin, LYVE-1, and VEGFR-3 (Figure 4C-F). IL-3 and LPS treatment for 6 or 24 hours activated NF-κB signaling as demonstrated by significant increases in p50, p65, and E-selectin, a known NF-κB–regulated gene (Figure 4C-D). After 6 hours of treatment with LPS and IL-3, VEGFR-3 was up-regulated by 6.2-fold (± 0.8-fold) and 4.4-fold (± 0.7-fold), respectively. After 24 hours of treatment with these stimuli, VEGFR-3 was up-regulated by 1.6-fold (± 2.4-fold) and 2.9-fold (± 0.2-fold), respectively (Figure 4E). In comparison, LYVE-1 was unchanged by IL-3 or down-regulated after 24 hours of LPS treatment (Figure 4F), attesting to the target specificity of NF-κB stimulation.

We hypothesized that IL-3– and LPS-induced VEGFR-3 would enhance LEC proliferation and migration to VEGFR-3–specific ligands, such as, VEGF-C152S.[39] To test this hypothesis, we measured proliferation and migration of RLECs stimulated by IL-3 or LPS alone or in combination with VEGF-C152S. VEGF-C152S, IL-3, or LPS significantly increased RLEC proliferation in a dose-dependent manner, with maximum increase of 2.2-, 1.8-, and 2.4-fold compared with control, respectively (Figure 4G-I). Preactivation with IL-3 or LPS followed 6 hours later by VEGF-C152S treatment significantly increased proliferation by 18% to 39% compared with individual cytokines (Figure 4J). IL-3, LPS, or VEGF-C152S also induced RLEC migration by 2.1-, 1.6-, and 1.8-fold (Figure 4K). LEC migratory response to VEGF-C152S increased up to 44% after pretreatment with IL-3 or LPS (Figure 4K). These results suggest that VEGFR-3 up-regulation by inflammatory stimuli mediating NF-κB activation enhances LEC responsiveness to VEGFR-3–specific ligands.
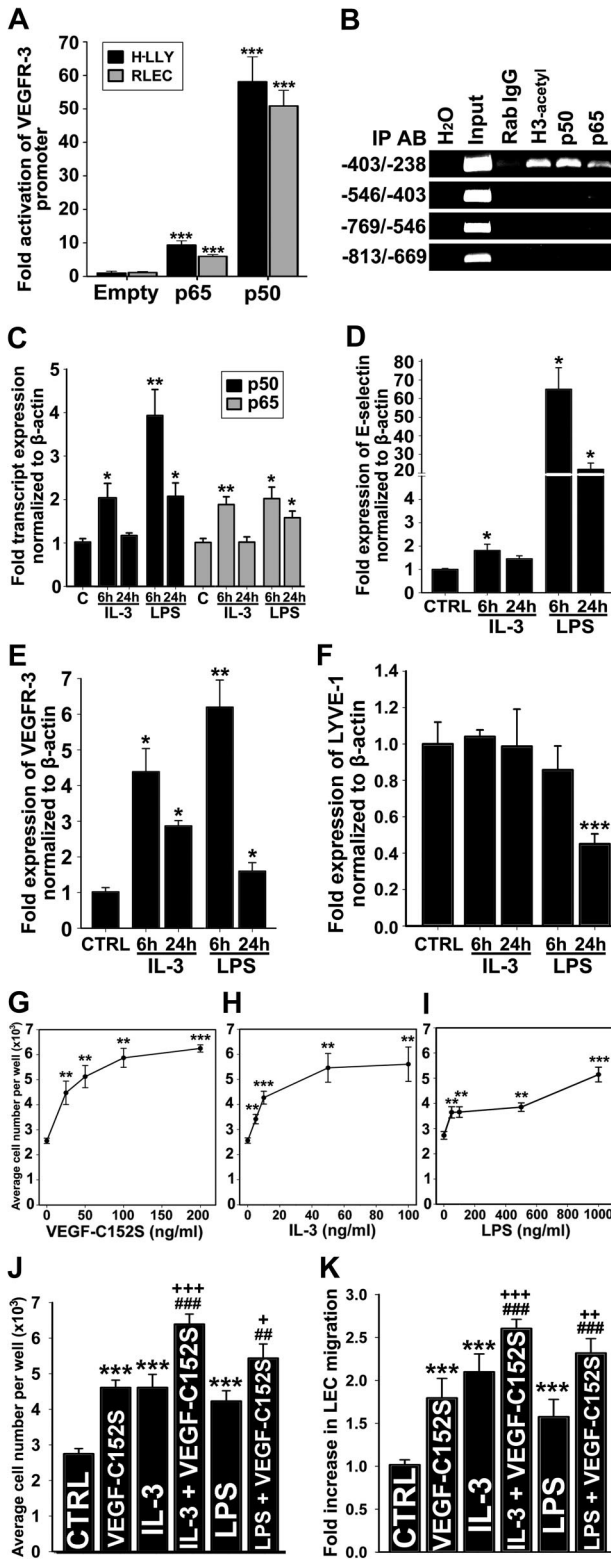
**Figure 4. NF-κB pathway up-regulates VEGFR-3 expression and activates lymphatic endothelial cells.** (A) VEGFR-3 promoter activity in RLECs and H-LLY cells cotransfected with VEGFR-3$^{-849/+55}$ and pCMV-Flag-p50, pCMV-Flag-p65, or empty control plasmids. Promoter activity is normalized per milligram of protein. Data presented for each cell line as the mean promoter activity ± SEM of 3 independent experiments performed in duplicate ± SEM (total n = 6 per experimental condition). ***$P < .001$ versus control as determined by Student unpaired $t$ test. (B) ChIP was performed using RLECs and anti-p65, -p50, and -acetylated histone H3 antibodies (positive control), or nonspecific rabbit IgG (negative control). Immunoprecipitated chromatin was visualized by PCR using primers either flanking (−403/−238 bp) or upstream of putative NF-κB binding sites (−813/−403 bp). Data are representative of 4 independent ChIP experiments with similar results. (C-F) qRT-PCR analysis of NF-κB p50 and p65 (C), E-selectin (D), VEGFR-3 (E), and LYVE-1 (F) mRNA expression in HDLECs$_{htert}$ treated with IL-3 (10 ng/mL) or LPS (100 ng/mL) for 6 or 24 hours. The relative expression of each target was normalized to β-actin. Data are presented as the mean values of 3 independent experiments ± SEM. *$P < .05$, **$P < .01$, and ***$P < .001$ versus control as determined by Student unpaired $t$ test. (G-I) RLEC proliferation induced by 72-hour exposure to VEGF-C152S (25-200 ng/mL; G), IL-3 (5-100 ng/mL; H), and LPS (50-1000 ng/mL; I). (J) Additive proliferative effects of RLECs treated with VEGF-C152S (100 ng/mL), IL-3 (10 ng/mL), or LPS (500 ng/mL) alone compared with pretreatment with IL-3 (10 ng/mL) or LPS (500 ng/mL) followed by stimulation with VEGF-C152S (100 ng/mL). (G-J) Data are presented as the average cell number of 3 independent experiments ± SEM (total n = 6 per condition). (K) Migration of RLECs induced by treatment with VEGF-C152S (200 ng/mL), IL-3 (10 ng/mL), or LPS (500 ng/mL) and combined treatment with IL-3 (10 ng/mL) and VEGF-C152S (200 ng/mL) or LPS (500 ng/mL) and VEGF-C152S (200 ng/mL). RLEC migration toward 0.25% FBS was used as a negative control. Data presented as average fold increase in RLEC migration ± SEM of 3 independent experiments. (J-K) *$P < .05$, **$P < .01$, and ***$P < .001$ versus control. ##$P < .01$ and ###$P < .001$ versus cytokine treatment alone. +$P < .05$, ++$P < .01$, and +++$P < .001$ versus VEGF-C152S treatment alone. All statistical tests were done by Student unpaired $t$ test.

**Figure 5. NF-κB signaling is required for VEGFR-3 expression in lymphatic endothelial cells.** (A) RLECs were transfected with the full-length VEGFR-3$^{-849/+55}$ promoter and treated with PDTC (0-1μM) or vehicle for 18 hours. Promoter activity was measured by luciferase assay and normalized to total protein per well. Note linear inhibition of VEGFR-3 promoter activity by PDTC determined by linear regression (r$^2$ shown on graph) of the mean promoter activity ± SEM of 3 independent experiments performed in duplicate (total n = 6 per condition). (B) VEGFR-3 transcript expression assayed by qRT-PCR in RLECs treated with PDTC (0-2μM) or vehicle. Data are presented as mean transcript expression normalized to β-actin of 3 independent experiments ± SEM (total n = 3 per condition). Inset shows a dose-dependent decrease of VEGFR-3 transcript detected by RT-PCR. (B-C) *$P$ < .05 versus control, **$P$ < .01 versus control, ***$P$ < .001 versus control, by Student unpaired $t$ test. (C) Western blot analysis of RLECs treated with PDTC (7.5μM), MG-132 (0.25μM), leptomycin B (10nM), or vehicle for 24 hours. β-Actin was used as a loading control. Vertical lines have been inserted to indicate repositioned gel lanes from blots presented in supplemental Figure 6, which show dose-dependent responses to NF-κB inhibitors. (D) Densitometric values demonstrate a statistically significant decrease in VEGFR-3 protein normalized to β-actin from RLECs treated with NF-κB inhibitors or vehicle for 24 hours. Experiments were performed in duplicate and data are presented as mean normalized per β-actin VEGFR-3 expression ± SEM; *$P$ < .05 versus control, by Student unpaired $t$ test. (E-G) H-LLY cells were transfected with p50- or p65-specific siRNA or scramble control siRNA for 48 hours and transcript expression for p50 (E), p65 (F), and VEGFR-3 (G) was determined by qRT-PCR. Data are presented as the mean transcript expression normalized to β-actin of 3 independent samples ± SEM (n = 3 per condition). Statistically significant differences were determined versus control, by Student unpaired $t$ test. $P$ values are displayed on the graphs.
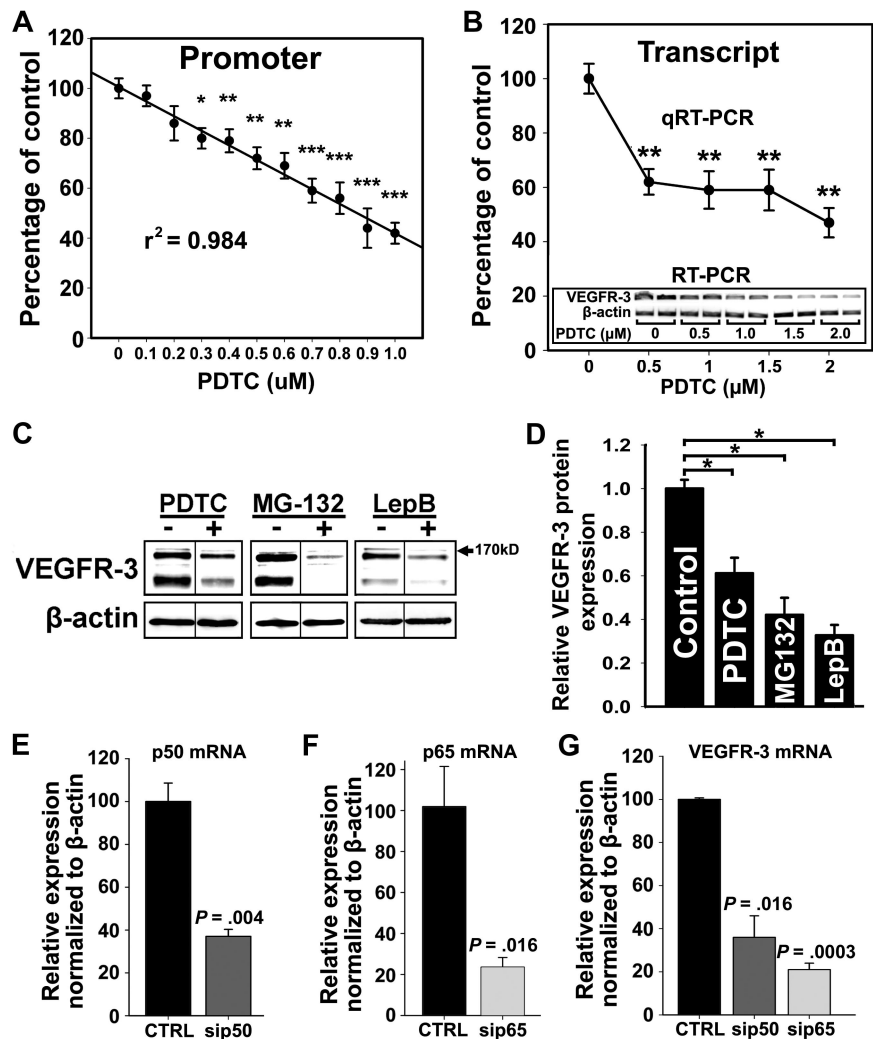
## Inhibition of NF-κB signaling represses VEGFR-3 expression in LECs

Because VEGFR-3 was elevated in inflamed lymphatic vessels (Figures 1-2) and upon forced expression of NF-κB proteins (Figure 4), we hypothesized that endogenous VEGFR-3 expression in LECs is maintained by constitutive NF-κB signaling. To test this hypothesis, we determined the effects of an NF-κB inhibitor PDTC[40] on VEGFR-3 expression at promoter, mRNA, and protein levels. PDTC-treated LECs demonstrated a dose-dependent reduction (up to 60%) of VEGFR-3 promoter activity and mRNA (Figure 5A-B). Constitutive expression and nuclear localization of p50 and p65 were also inhibited by PDTC, which coincided with decreased VEGFR-3 expression (supplemental Figure 5). Neither cell viability (supplemental Figure 6) nor expression of NF-κB–independent targets (eg, β-actin) was affected by PDTC at the tested concentrations (Figure 5B inset). This effect was reproduced by 2 other inhibitors: MG-132, a blocker of IκB-α degradation,[40] and leptomycin B, an inhibitor of NF-κB nuclear transport.[41] Western blot showed up to 70% reduction of VEGFR-3 expression by all inhibitors in a dose-dependent manner (Figure 5C-D). Drug concentrations that repressed VEGFR-3 protein expression were at least 10-fold below the median inhibitory concentration values for LECs (supplemental Figure 6).

NF-κB regulation of VEGFR-3 expression was also confirmed by target-specific knockdown of NF-κB subunits. H-LLY cells

were transfected with siRNA targeting p50 or p65 or scrambled control siRNA. qRT-PCR performed 48 hours after transfection showed 50% to 70% knockdown of p50 and p65 (Figure 5E-F) and a corresponding 50% to 80% reduction in VEGFR-3 transcripts (Figure 5G). Collectively, these data suggest that NF-κB is involved in regulation of endogenous VEGFR-3 expression.

## The VEGFR-3 promoter is activated by Prox1

Prox1 has been reported to induce VEGFR-3 expression in cultured endothelial cells.[18,20] However, Prox1 regulates more than 90 genes[20] and transactivation of the VEGFR-3 promoter by Prox1 has not been previously shown. To determine whether Prox1 transcriptionally regulates VEGFR-3, LECs were cotransfected with VEGFR-3$^{-849/+55}$ promoter and escalating concentrations (0-0.5 μg) of a Prox1-encoding or empty vector followed by measurement of luciferase activity. Relative to empty-vector control, overexpression of Prox1 increased VEGFR-3$^{-849/+55}$ activity in a linear dose-dependent manner by 76-fold and 7-fold in H-LLY and RLECs, respectively (Figure 6A-B).

Several putative Prox1 binding sites, analogous to published consensus sequences (CA/tc/tNNCT/c and TA/tAGNC/tN[42]), are present in both human and rat VEGFR-3 promoters. ChIP assay in RLECs showed that the region containing consensus Prox1 binding sites (−403/−238 bp) was immunoprecipitated by anti-Prox1 antibody (Figure 6C, supplemental Figure 7). Prox1 antibodies did
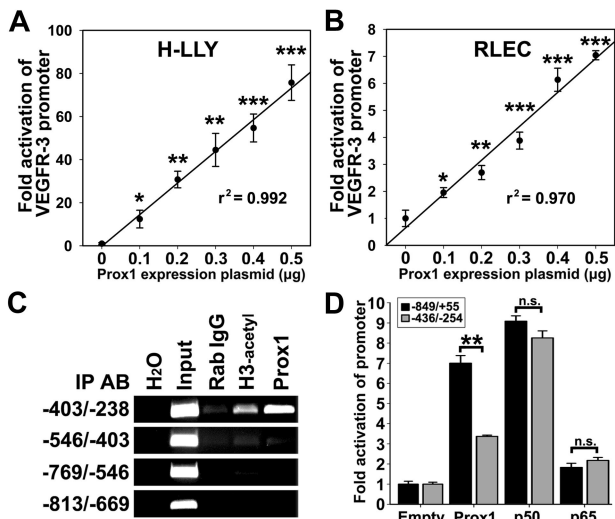
**Figure 6. Prox1 directly activates the VEGFR-3 promoter.** VEGFR-3$^{-849/+55}$ promoter plasmid was cotransfected with pCMV-Prox1 plasmid (0-0.5 μg) in H-LLY cells (A) and RLECs (B). Promoter activity was measured by luciferase assay and normalized per milligram of protein. Note linear response to Prox1 transactivation in both cell lines as determined by linear regression ($r^2$ shown on graph) of the mean promoter activity ± SEM of 3 independent experiments performed in duplicate (n = 6 per condition; A-B). (A-B) *$P < .05$ versus control, **$P < .01$ versus control, ***$P < .001$ versus control, by Student unpaired $t$ test. (C) ChIP analysis of the VEGFR-3 promoter was performed on RLECs as described in the legend for Figure 4. Immunoprecipitated chromatin was visualized by PCR with primers flanking transcription factor binding sites (−403/−238 bp) or upstream of binding sites (−813/−403 bp). Data are representative of 3 independent ChIP experiments with similar results. (D) Fold activation of a truncated VEGFR-3 promoter (−436/−254) was compared with the full-length VEGFR-3$^{-849/+55}$. RLECs were cotransfected with 0.5 μg of VEGFR-3$^{-849/+55}$ or VEGFR-3$^{-436/-254}$ promoter plasmids and 0.5 μg of pCMV-Prox1, pCMV-Flag-p50, pCMV-Flag-p65, or empty control plasmid. Promoter activity is normalized per milligram of protein. Data are presented as the mean promoter activity of 3 independent experiments performed in duplicate ± SEM (total n = 6 per experimental condition). ns denotes nonsignificant changes. **$P < .01$ versus control as determined by Student unpaired $t$ test.

not pull down other flanking promoter DNA, indicating specific interaction between Prox1 and the VEGFR-3 promoter within a promoter segment that was also bound by NF-κB (Figure 4B). To test whether this region is crucial for promoter activation, RLECs were cotransfected with a construct encoding bases −436 to −254 (VEGFR-3$^{-436/-254}$) and pCMV-Prox1, pCMV-Flag-p50, pCMV-Flag-p65, or empty plasmids. VEGFR-3$^{-849/+55}$ and VEGFR-3$^{-436/-254}$ were identically activated by p50 and p65, whereas Prox1 fold activation of VEGFR-3$^{-436/-254}$ was reduced approximately by half compared with the full-length promoter (Figure 6D). This suggests that full activation by Prox1 might require interaction with additional sites outside of the −436/−254-bp region.

### NF-κB regulates Prox1 expression in LECs

We found that forced expression of Prox1 activated VEGFR-3 promoter in vitro and both Prox1 and VEGFR-3 are induced by inflammation in vivo with Prox1 up-regulation preceding that of VEGFR-3 (Figure 2). This suggested that NF-κB might first up-regulate Prox1 followed by cooperative regulation of VEGFR-3. To test this hypothesis, the level of Prox1 expression was quantified by qRT-PCR after 6-hour stimulation by IL-3 (10 ng/mL), conditions that increased VEGFR-3 expression (Figure 4E). IL-3 significantly increased Prox1 by 2-fold ($P < .01$, Figure 7A), implicating Prox1 as a downstream target of NF-κB.

We next investigated the effects of NF-κB inhibitors on Prox1 expression. PDTC suppressed Prox1 mRNA by approximately

60% (Figure 7B), suggesting that Prox1 transcription requires NF-κB. Western blot showed that PDTC, MG-132, and leptomycin B all significantly repressed Prox1 expression (Figure 7C). Moreover, p50 and p65 siRNA but not scrambled control also decreased Prox1 expression by 60% (Figure 7D), corroborating the hypothesis that NF-κB regulates Prox1 in LECs.

### Prox1 and NF-κB synergistically activate the VEGFR-3 promoter

Cultured LECs express high levels of Prox1 and p50, making it difficult to evaluate the contributions of these factors to VEGFR-3 transcription. To test whether Prox1 and NF-κB cooperate in activation of the VEGFR-3 promoter, we used Prox1-negative nonendothelial (HEK293) and endothelial (HULEC) lines. Similar results were obtained in both lines cotransfected with Prox1 (Figure 7E-F insets), the full-length VEGFR-3$^{-849/+55}$ promoter and Flag-p50, Flag-p65, or empty vector. In the absence of Prox1, p50 weakly activated the VEGFR-3 promoter, whereas p65 had no effect. Prox1 combined with p65 did not increase promoter activity compared with Prox1 alone. In contrast, Prox1 combined with p50 activated the VEGFR-3 promoter 22.3-fold (± 0.7-fold) and 66.9-fold (± 3.8-fold) over the vector control in HEK293 cells and HULECs, respectively (Figure 7E-F). Combination of these plasmids had no effect on the activity of NF-κB–independent ubiquitin C (UBC) or phosphoglycerate kinase (PGK) promoters. The activity of a truncated VEGFR-3$^{-118/+55}$ promoter in response to Prox1, p50, and p65 alone or in combination was significantly reduced compared with the responses of the full-length VEGFR-3$^{-849/+55}$ (Figure 7G, supplemental Figure 8). These results confirm the functionality of the region beyond −118 bp and suggest that Prox1 and NF-κB p50 synergistically activate the VEGFR-3 promoter.

## Discussion

### Inflammation and NF-κB signaling up-regulate VEGFR-3 expression during lymphangiogenesis

Inflammation is the main physiologic event that evokes formation of new lymphatic vessels in adulthood.[43] Although the role of inflammation in induction of lymphangiogenesis has long been recognized, the underlying molecular mechanisms remained undefined. We present novel evidence that inflammation-induced NF-κB signaling precedes lymphatic-specific up-regulation of VEGFR-3 and that NF-κB activates VEGFR-3 transcription in cultured LECs (Figures 1-2,4). Moreover, our data show that NF-κB–dependent mediators, IL-3 and LPS, increase VEGFR-3 expression and responsiveness of LECs to VEGFR-3–activating factors (Figure 4). Collectively, these results suggest that LEC stimulation by NF-κB–dependent cytokines amplifies the lymphangiogenic signals by increasing VEGFR-3 expression.

In vivo analysis demonstrated that up-regulation of VEGFR-3 on preexisting vessels preceded formation of new LYVE-1$^+$ vessels by several days (Figures 1-2), suggesting that elevated VEGFR-3 expression is crucial for induction of lymphangiogenesis. This is consistent with previous reports demonstrating the paramount role of VEGFR-3 for LEC activation and inflammatory lymphangiogenesis as shown by blocking this receptor in models of LPS-induced peritonitis,[44] chronic airway infection,[9] wound healing,[16] and cancer.[17] VEGFR-3 ligands, VEGF-C/-D, are highly expressed during inflammation by infiltrating immune cells, such as CD11b$^+$ macrophages.[44,45] The abundant expression of VEGF-C/-D at inflamed sites suggests that lymphangiogenesis might be restricted by limited VEGFR-3 expression on preexisting

lymphatic vessels rather than by ligand availability. A low density of VEGFR-3 receptors may result in self-limiting lymphangiogenesis due to receptor saturation and internalization. In contrast, high level of VEGFR-3 expression might be induced by inflammation due to sustained cytokine production and continuous activation of NF-κB in LECs.

### Prox1 is up-regulated during inflammation and mediates VEGFR-3 expression

Prox1 is an essential mediator of embryonic lymphangiogenesis,[18,20] but little is known about its functions in adulthood. We present novel evidence that Prox1 expression is rapidly increased after the onset of inflammation preceding both VEGFR-3 up-regulation and lymphangiogenesis (Figures 1-2). We also showed that the NF-κB–dependent cytokine, IL-3, up-regulates Prox1 in adult LECs, which is consistent with prior reports that IL-3 induced

Prox1 expression in adult BECs.[22] Elevated expression of Prox1 and VEGFR-3 has also been shown in Kaposi sarcoma.[46] However, the latter finding could be construed as induction by tumor-derived factors rather than by sustained NF-κB activation. In comparison, we report here lymphatic-specific induction of Prox1 by NF-κB–dependent cytokines and suppression of Prox1 by NF-κB–specific inhibitors. These data suggest that Prox1 might regulate responsiveness to inflammation in adult LECs.

Prox1 regulates acquisition of lymphatic phenotype during embryogenesis[18] and transdifferentiation of adult BECs to LECs.[18,20] Up-regulation of Prox1 induces VEGFR-3,[18,20] whereas silencing Prox1 suppresses VEGFR-3 expression.[21] Our data suggest that Prox1 induces VEGFR-3 expression through promoter transactivation as indicated by ChIP and a dose-dependent increase in promoter activity (Figure 6). These data identify Prox1 as a potential downstream target of NF-κB and a regulator of VEGFR-3 expression under inflammatory conditions.

### VEGFR-3 transcription is predominantly regulated by NF-κB p50 that might cooperate with Prox1

We show that NF-κB p50, rather than p65, is the predominant activator of VEGFR-3 (Figures 4,7). Preferential activation by p50 was reported for other promoters including Bcl-2[47] and PDGF-A.[48] In contrast, promoters of some NF-κB responsive genes (eg, TNF-α and IL-8) are suppressed by p50 homodimers.[49] This suggests that p50 can function as a transcriptional activator or repressor depending on cellular context, sequence of the response element, and transcriptional cofactors. Because p50 lacks a consensus transactivation domain,[24] p50-driven transcription requires coactivators, such as Bcl-3[47] or C/EBP proteins,[50] that might be present in LECs. Both Prox1 and p50 have been shown to interact with the transcriptional coactivator, CBP/p300,[50] suggesting that such protein-protein interaction might account for synergistic activation of the VEGFR-3 promoter (Figure 7). Prox1 might also
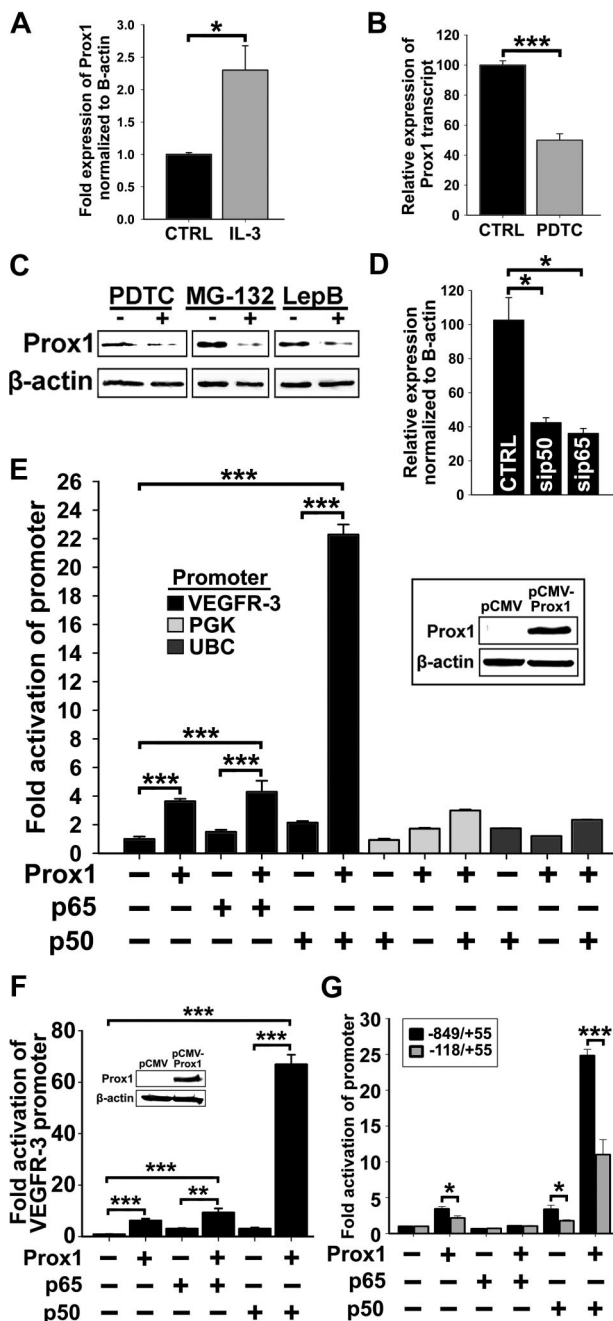


**Figure 7. The p50 subunit of NF-κB up-regulates Prox1, and both p50 and Prox1 synergistically regulate VEGFR-3 expression.** (A) qRT-PCR analysis of Prox1 transcripts in HDLECs$_{htert}$ treated with IL-3 (10 ng/mL) for 6 hours. (B) qRT-PCR analysis of Prox1 transcripts in RLECs treated with PDTC (2.5μM) for 24 hours. (A-B) Data are presented as β-actin normalized mean transcript expression of 3 independent experiments performed in duplicate ± SEM (total: n = 6 per condition). (C) Prox1 detected by Western blot of nuclear extracts from RLECs treated with PDTC (5μM), MG-132 (250nM), leptomycin B (10nM), or vehicle alone. β-Actin was used as a loading control. Representative data are shown from 1 of 3 experiments. (D) qRT-PCR analysis of Prox1 transcript in H-LLY transfected with p50 and p65 siRNA. Data are presented as the mean transcript expression normalized to β-actin ± SEM derived from 3 independent samples. (E) Prox1-negative nonendothelial line HEK293 was transfected with VEGFR-3$^{-849/+55}$ promoter plasmid and pCMV-Flag-p50 or pCMV-Flag-p65 plasmids and cotransfected with pCMV-Prox1 or empty vector (0.25 μg of each plasmid). VEGFR-3 promoter activity was normalized to total milligram of protein. Inset confirms lack of Prox1 in control HEK293 and forced expression in transfected cells. Activation of VEGFR-3 promoter by coexpression of p50 and Prox1 was compared with the effect on NF-κB–independent promoters for phosphoglycerate kinase (PGK) and ubiquitin C (UBC) examined under the same conditions. Data presented as the mean promoter activity ± SEM of 3 independent experiments performed in triplicate (total n = 9 per condition). (F) Prox1-negative blood vascular endothelial line, HULEC, was transfected with VEGFR-3$^{-849/+55}$ promoter expression and pCMV-Flag-p50 or pCMV-Flag-p65 plasmids and cotransfected with pCMV-Prox1 or empty vector, as described in panel E. The analysis of the VEGFR-3 promoter activity was performed as described in panel E. Data are presented as the mean VEGFR-3 promoter activity ± SEM derived from 3 independent experiments performed in quadruplicate (total n = 12 per condition). (G) Fold activation of the full-length (−849/+55 bp) and truncated (−118/+55 bp) VEGFR-3 promoters was compared after cotransfection with pCMV-Prox1, pCMV-Flag-p50, and pCMV-Flag-p65 alone or in combination as described in panel E. Data are presented as the mean VEGFR-3 promoter activity ± SEM derived from 3 independent experiments. *P < .05, **P < .01, and ***P < .001 versus control, as determined by Student unpaired t test.

be a lymphatic-specific coactivator of p50, which would account for the weak transactivation of the VEGFR-3 promoter by p50 in Prox1-negative BECs (Figure 7) and the lack of VEGFR-3 up-regulation on inflamed blood vasculature (supplemental Figure 3). This is consistent with overlapping peaks and protein kinetics of p-p50 and Prox1 observed in vivo (Figure 2), suggesting that Prox1 might confer lymphatic specificity to ubiquitously activated NF-κB signaling during inflammation. Thus, the cooperative role of Prox1 with p50 in regulation of VEGFR-3 transcription could be 2-fold: to amplify p50 signaling and to impart lymphatic specificity to activated NF-κB, promoting lymphangiogenesis-required gene expression.

In summary, we demonstrate that increased Prox1 and VEGFR-3 expression precedes lymphangiogenesis in vivo. Increased expression of VEGFR-3 is likely mediated by Prox1 and NF-κB binding to its promoter. Prox1 induced by NF-κB synergizes with p50 in activation of the promoter, suggesting a complex interplay between ubiquitous and lymphatic-specific proteins. Future delineation of these mechanisms might identify targets for therapeutic control of abnormal lymphangiogenesis induced at chronically inflamed sites and malignancy.

## Acknowledgments

## Authorship

Contribution: M.J.F. designed research, performed or supervised experiments, analyzed and interpreted data, and wrote the paper; A.W. contributed vital new reagents and wrote the paper; K.L.H. performed siRNA experiments; C.I. and K.M. contributed vital new reagents; R.E.N. and M.S.P. contributed HDLECs_{htert}; D.C.Z. contributed RLECs; and S.R. designed research, supervised experiments, analyzed and interpreted data, and wrote the paper.

Conflict-of-interest disclosure: The authors declare no competing financial interests.

Correspondence: Sophia Ran, Department of Medical Microbiology, Immunology and Cell Biology, Southern Illinois University School of Medicine, 801 N Rutledge, Springfield, IL 62794-9626; e-mail: sran@siumed.edu.

## References

1. Swartz MA, Hubbell JA, Reddy ST. Lymphatic drainage function and its immunological implications: from dendritic cell homing to vaccine design. *Semin Immunol.* 2008;20(2):147-156.

2. Shin WS, Rockson SG. Animal models for the molecular and mechanistic study of lymphatic biology and disease. *Ann N Y Acad Sci.* 2008; 1131:50-74.

3. Jamieson T, Cook DN, Nibbs RJ, et al. The chemokine receptor D6 limits the inflammatory response in vivo. *Nat Immunol.* 2005;6(4):403-411.

4. Achen MG, Stacker SA. Molecular control of lymphatic metastasis. *Ann N Y Acad Sci.* 2008;1131: 225-234.

5. Veikkola T, Jussila L, Makinen T, et al. Signalling via vascular endothelial growth factor receptor-3 is sufficient for lymphangiogenesis in transgenic mice. *EMBO J.* 2001;20(6):1223-1231.

6. Kaipainen A, Korhonen J, Mustonen T, et al. Expression of the fms-like tyrosine kinase 4 gene becomes restricted to lymphatic endothelium during development. *Proc Natl Acad Sci U S A.* 1995;92(8):3566-3570.

7. Whitehurst B, Flister MJ, Bagaitkar J, et al. Anti-VEGF-A therapy reduces lymphatic vessel density and expression of VEGFR-3 in an orthotopic breast tumor model. *Int J Cancer.* 2007;121(10): 2181-2191.

8. Paavonen K, Puolakkainen P, Jussila L, Jahkola T, Alitalo K. Vascular endothelial growth factor receptor-3 in lymphangiogenesis in wound healing. *Am J Pathol.* 2000;156(5):1499-1504.

9. Baluk P, Tammela T, Ator E, et al. Pathogenesis of persistent lymphatic vessel hyperplasia in chronic airway inflammation. *J Clin Invest.* 2005; 115(2):247-257.

10. Kunstfeld R, Hirakawa S, Hong YK, et al. Induction of cutaneous delayed-type hypersensitivity reactions in VEGF-A transgenic mice results in chronic skin inflammation associated with persistent lymphatic hyperplasia. *Blood.* 2004;104(4): 1048-1057.

11. Zhang Q, Lu Y, Proulx ST, et al. Increased lymphangiogenesis in joints of mice with inflammatory arthritis. *Arthritis Res Ther.* (http://arthritis-research.com/content/pdf/ar2326.pdf). 2007;9(6): R118.

12. Maruyama K, Ii M, Cursiefen C, et al. Inflammation-induced lymphangiogenesis in the cornea arises from CD11b-positive macrophages. *J Clin Invest.* 2005;115(9):2363-2372.

13. Cursiefen C, Chen L, Borges LP, et al. VEGF-A stimulates lymphangiogenesis and hemangiogenesis in inflammatory neovascularization via macrophage recruitment. *J Clin Invest.* 2004; 113(7):1040-1050.

14. Iwata C, Kano MR, Komuro A, et al. Inhibition of cyclooxygenase-2 suppresses lymph node metastasis via reduction of lymphangiogenesis. *Cancer Res.* 2007;67(21):10181-10189.

15. Ristimäki A, Narko K, Enholm B, Joukov V, Alitalo K. Proinflammatory cytokines regulate expression of the lymphatic endothelial mitogen vascular endothelial growth factor-C. *J Biol Chem.* 1998; 273(14):8413-8418.

16. Goldman J, Rutkowski JM, Shields JD, et al. Cooperative and redundant roles of VEGFR-2 and VEGFR-3 signaling in adult lymphangiogenesis. *FASEB J.* 2007;21(4):1003-1012.

17. Roberts N, Kloos B, Cassella M, et al. Inhibition of VEGFR-3 activation with the antagonistic antibody more potently suppresses lymph node and distant metastases than inactivation of VEGFR-2. *Cancer Res.* 2006;66(5):2650-2657.

18. Hong YK, Harvey N, Noh YH, et al. Prox1 is a master control gene in the program specifying lymphatic endothelial cell fate. *Dev Dyn.* 2002; 225(3):351-357.

19. Wigle JT, Harvey N, Detmar M, et al. An essential role for Prox1 in the induction of the lymphatic endothelial cell phenotype. *EMBO J.* 2002;21(7): 1505-1513.

20. Petrova TV, Makinen T, Makela TP, et al. Lymphatic endothelial reprogramming of vascular endothelial cells by the Prox-1 homeobox transcription factor. *EMBO J.* 2002;21(17):4593-4599.

21. Mishima K, Watabe T, Saito A, et al. Prox1 induces lymphatic endothelial differentiation via integrin alpha9 and other signaling cascades. *Mol Biol Cell.* 2007;18(4):1421-1429.

22. Gröger M, Loewe R, Holnthoner W, et al. IL-3 induces expression of lymphatic markers Prox-1 and podoplanin in human endothelial cells. *J Immunol.* 2004;173(12):7161-7169.

23. Karin M. Nuclear factor-kappaB in cancer development and progression. *Nature.* 2006;441(7092):431-436.

24. Beinke S, Ley SC. Functions of NF-kappaB1 and NF-kappaB2 in immune cell biology. *Biochem J.* 2004;382(pt 2):393-409.

25. Kiriakidis S, Andreakos E, Monaco C, et al. VEGF expression in human macrophages is NF-kappaB-dependent: studies using adenoviruses expressing the endogenous NF-kappaB inhibitor IkappaBalpha and a kinase-defective form of the IkappaB kinase 2. *J Cell Sci.* 2003; 116(pt 4):665-674.

26. Tsai PW, Shiah SG, Lin MT, Wu CW, Kuo ML. Up-regulation of vascular endothelial growth factor C in breast cancer cells by heregulin-beta 1: a critical role of p38/nuclear factor-kappa B signaling pathway. *J Biol Chem.* 2003;278(8):5750-5759.

27. Wilber A, Frandsen JL, Wangensteen KJ, et al. Dynamic gene expression after systemic delivery of plasmid DNA as determined by in vivo bioluminescence imaging. *Hum Gene Ther.* 2005;16(11): 1325-1332.

28. Whitehurst B, Eversgerd C, Flister M, et al. Molecular profile and proliferative responses of rat lymphatic endothelial cells in culture. *Lymphat Res Biol.* 2006;4(3):119-142.

29. Nisato RE, Harrison JA, Buser R, et al. Generation and characterization of telomerase-transfected human lymphatic endothelial cells with an extended life span. *Am J Pathol.* 2004; 165(1):11-24.

30. Tammela T, Saaristo A, Lohela M, et al. Angiopoietin-1 promotes lymphatic sprouting and hyperplasia. *Blood.* 2005;105(12):4642-4648.

31. National Center for Biotechnology Information. GenBank. http://www.ncbi.nlm.nih.gov/Genbank. Accessed February 14, 2007.

32. Genomatix. MatInspector. http://www.genomatix.de/products/MatInspector/index.html. Accessed March 02, 2007.

33. Laderach D, Compagno D, Danos O, Vainchenker W, Galy A. RNA interference shows critical requirement for NF-kappa B p50 in the production of IL-12 by human dendritic cells. *J Immunol.* 2003;171(4):1750-1757.

34. Surabhi RM, Gaynor RB. RNA interference directed against viral and cellular targets inhibits human immunodeficiency virus type 1 replication. *J Virol.* 2002;76(24):12963-12973.

35. Kilic N, Oliveira-Ferrer L, Neshat-Vahid S, et al. Lymphatic reprogramming of microvascular endothelial cells by CEA-related cell adhesion molecule-1 via interaction with VEGFR-3 and Prox1. *Blood.* 2007;110(13):4223-4233.

36. Oka M, Iwata C, Suzuki HI, et al. Inhibition of endogenous TGF-{beta} signaling enhances lymphangiogenesis. *Blood.* 2008;111(9):4571-4579.

37. Srinivasan RS, Dillard ME, Lagutin OV, et al. Lineage tracing demonstrates the venous origin of the mammalian lymphatic vasculature. *Genes Dev.* 2007;21(19):2422-2432.

38. Iljin K, Karkkainen MJ, Lawrence EC, et al. VEGFR3 gene structure, regulatory region, and sequence polymorphisms. *FASEB J.* 2001;15(6):1028-1036.

39. Kirkin V, Mazitschek R, Krishnan J, et al. Characterization of indolinones which preferentially inhibit VEGF-C- and VEGF-D-induced activation of VEGFR-3 rather than VEGFR-2. *Eur J Biochem.* 2001;268(21):5530-5540.

40. Dai Y, Rahmani M, Grant S. Proteasome inhibitors potentiate leukemic cell apoptosis induced by the cyclin-dependent kinase inhibitor flavopiridol through a SAPK/JNK- and NF-kappaB-dependent process. *Oncogene.* 2003;22(46):7108-7122.

41. Walsh MD Jr, Hamiel CR, Banerjee A, et al. Exportin 1 inhibition attenuates nuclear factor-kappaB-dependent gene expression. *Shock.* 2008;29(2):160-166.

42. Chen X, Taube JR, Simirskii VI, Patel TP, Duncan MK. Dual roles for Prox1 in the regulation of the chicken betaB1-crystallin promoter. *Invest Ophthalmol Vis Sci.* 2008;49(4):1542-1552.

43. Mouta C, Heroult M. Inflammatory triggers of lymphangiogenesis. *Lymphat Res Biol.* 2003;1(3):201-218.

44. Kataru RP, Jung K, Jang C, et al. Critical role of CD11b+ macrophages and VEGF in inflammatory lymphangiogenesis, antigen clearance, and inflammation resolution. *Blood.* 2009;113(22):5650-5659.

45. Kang S, Lee SP, Kim KE, et al. Toll-like receptor 4 in lymphatic endothelial cells contributes to LPS-induced lymphangiogenesis by chemotactic recruitment of macrophages. *Blood.* 2009;113(11):2605-2613.

46. Hong YK, Foreman K, Shin JW, et al. Lymphatic reprogramming of blood vascular endothelium by Kaposi sarcoma-associated herpesvirus. *Nat Genet.* 2004;36(7):683-685.

47. Kurland JF, Kodym R, Story MD, et al. NF-kappaB1 (p50) homodimers contribute to transcription of the bcl-2 oncogene. *J Biol Chem.* 2001;276(48):45380-45386.

48. Aizawa K, Suzuki T, Kada N, et al. Regulation of platelet-derived growth factor-A chain by Kruppel-like factor 5: new pathway of cooperative activation with nuclear factor-kappaB. *J Biol Chem.* 2004;279(1):70-76.

49. Tong X, Yin L, Washington R, Rosenberg DW, Giardina C. The p50-p50 NF-kappaB complex as a stimulus-specific repressor of gene activation. *Mol Cell Biochem.* 2004;265(1-2):171-183.

50. Chen Q, Dowhan DH, Liang D, Moore DD, Overbeek PA. CREB-binding protein/p300 coactivation of crystallin gene expression. *J Biol Chem.* 2002;277(27):24081-24089.